Tetrahedron 64 (2008) 7937–7943

Contents lists available at ScienceDirect

Tetrahedron

journal homepage: www.elsevier.com/locate/tet

Mechanistic insights on the site selectivity in successive 1,3-dipolar cycloadditions to *meso*-tetraarylporphyrins

G. Jiménez-Osés [a,*], J.I. García [a], A.M.G. Silva [b], A.R.N. Santos [b], A.C. Tomé [b], M.G.P.M.S. Neves [b], J.A.S. Cavaleiro [b]

[a] *Departamento de Química Orgánica, Instituto de Ciencia de Materiales de Aragón, Instituto Universitario de Catálisis Homogénea, Universidad de Zaragoza-CSIC, E-50009 Zaragoza, Spain*
[b] *Departamento de Química, Universidade de Aveiro, 3810-193 Aveiro, Portugal*

ARTICLE INFO

Article history:
Received 14 February 2008
Received in revised form 5 June 2008
Accepted 6 June 2008
Available online 10 June 2008

Keywords:
Porphyrins
Bacteriochlorins
Isobacteriochlorins
Site selectivity
1,3-Dipolar cycloadditions
DFT calculations
Solvent effects
Aromaticity

ABSTRACT

A DFT study on site selectivity in successive 1,3-dipolar cycloadditions of *meso*-tetraarylporphyrins with azomethine ylide and *N*-methylnitrone has been carried out. The calculation of the thermodynamic stability of both ylide and nitrone-derived adducts reveals that bacteriochlorins are more stable and have stronger aromatic character than isobacteriochlorins. Calculations of whole reaction pathways show that cycloadditions of azomethine ylide on porphyrin and its derived chlorin are irreversible and hence kinetically controlled. Solvent influence on the site selectivity of this reaction has also been considered, and appears to be decisive in controlling the site selectivity. In contrast, cycloadditions of nitrone over porphyrin and chlorin are clearly reversible, pointing to a thermodynamic control of these reactions.

1. Introduction

In recent years, great effort has been put forth towards the development and improvement of new methods to convert porphyrins into dihydroporphyrins (chlorins) and tetrahydroporphyrins (isobacteriochlorins and bacteriochlorins). This is mainly due to the potential use of such compounds in several scientific areas, with a special emphasis in medicine. Present medicinal formulations already being used in several countries include porphyrin derivatives as photosensitisers for the photodetection and treatment (photodynamic therapy, PDT) of cancer cells and for the treatment of the age-related macular degeneration. Amphiphilic structural features, simple synthesis and absorptions near the infrared region are requirements to be fulfilled by any new potential photosensitiser; good books and reviews related to this subject have been published.[1] Particularly, for a deep penetration of the light into tissue is required a photosensitiser with a strong absorption in the visible region near or above 650 nm, like chlorins and bacteriochlorins. Bacteriochlorins with significant absorptions at >700 nm do play a key role in such processes.

Several groups have shown that Diels–Alder reactions and 1,3-dipolar cycloadditions can be excellent tools for preparing novel derivatives containing such macrocyclic features.[2–4] In addition, the high versatility and the regio- and stereoselectivity found in those reactions[5] can be used to prepare new porphyrinic compounds with well-defined stereochemistry.

The 1,3-dipolar cycloaddition (1,3-DC) reactions have been widely used as a simple and versatile method for construction of five-membered heterocyclic rings, many of them with extensive laboratory, industrial and medicinal applications.[5] In the 1,3-DC reactions of an 1,3-dipole with an 1,2-disubstituted alkene, two or more new stereogenic centres can be formed in the adduct; the majority of these reactions are diastereoselective.

In the case of porphyrins, the 1,3-DC reaction of azomethine ylide **2y** with porphyrin **1** can afford only one monoadduct, chlorin **3y** (*meso* compound) as shown in Scheme 1. However, the situation becomes more complex when a second cycloaddition is performed on the resulting chlorin **3y**. In this case, the reaction can lead to four different bisadducts, namely isobacteriochlorins **5′yc** and **5′yt**, and bacteriochlorins **4yc** and **4yt**, depending on the cycloaddition occurring on the adjacent or opposite pyrrolic double bonds (site

* Corresponding author. Tel.: +34 976 762271; fax: +34 976 762070.
E-mail address: gjimenez@unizar.es (G. Jiménez-Osés).

0040-4020/$ – see front matter © 2008 Elsevier Ltd. All rights reserved.
doi:10.1016/j.tet.2008.06.018

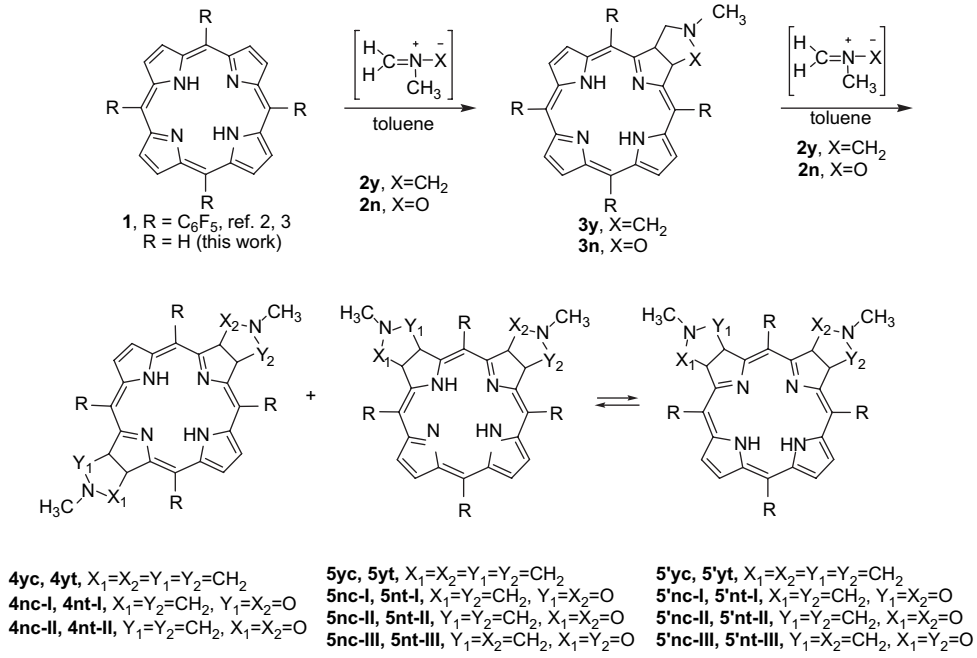

Scheme 1. Reaction of porphyrin **1** with azomethine ylide **2y** and *N*-methylnitrone **2n** showing the products distribution including different tautomers, stereoisomers and site isomers considered in this work.

selectivity) and leading to cis or trans isomers (stereoselectivity). When the non-symmetrical nitrone **2n** is used instead of the symmetrical azomethine ylide **2y**, the 1,3-DC reaction with porphyrin **1** affords chlorin **3n** as a racemic mixture (Scheme 1). When a second cycloaddition is performed on chlorin **3n**, a complex mixture of bisadducts can be obtained since the nitrone **2n** can react in three different relative orientations with regard to the isoxazolidine ring of chlorin **3n** (regioselectivity), on two different double bonds (site selectivity), and affording cis and trans isomers (stereoselectivity). Experimentally, the reaction of azomethine ylide **2y** with porphyrin **1**, carried out in refluxing toluene during 15 h, afforded chlorin **3y** in 61% yield and isobacteriochlorins **5′y** in 11% yield together with traces of bacteriochlorins **4y**.[2a] In marked contrast, the reaction of *N*-methylnitrone **2n** with porphyrin **1**, carried out in toluene at 60 °C during 5 days, afforded chlorin **3n** in 72% yield and bacteriochlorins **4n** in small amount (16%).[3a]

With these evidences in mind, we decided to carry out a computational and experimental mechanistic studies of the reaction of *meso*-tetraarylporphyrins with the two 1,3-dipoles, trying to explain the surprising different behaviour experimentally observed.

2. Results and discussion

In order to reduce the complexity of the system, we chose the *meso*-unsubstituted porphyrin **1** (R=H), azomethine ylide **2y** and *N*-methylnitrone **2n** as convenient reactants for the theoretical study. The aryl groups of *meso*-tetrasubstituted porphyrins were simplified to hydrogen atoms in the theoretical model, because no significant changes in site- or stereoselectivities were expected. Cis and trans isomers were denoted with labels **c** and **t**, respectively, whereas regioisomers were denoted with labels **I**, **II** and **III**. According to preliminary calculations and agreeing with previous studies,[6] and experimental observations,[2,3] we considered only the most stable tautomers for general discussion, i.e., only **4** tautomers in the case of bacteriochlorins, and both **5** and **5′** tautomers (which are very close in energy) in the case of isobacteriochlorins (Scheme 1).

2.1. Reaction thermodynamics

As a first approximation, we calculated the thermodynamic stability of the final products. Figure 1 shows some representative structures of bacterio- and isobacteriochlorins in two tautomeric forms (all the calculated structures can be found in the Supplementary data). As can be observed in this plot, the two new rings are almost identical in each compound due to symmetry. In terms of energy, and as can be seen in Table 1, bacteriochlorins **4y** and **4n** are the most stable isomers (by more than 4 kcal mol^{-1} lower in energy) in both ylide and nitrone-derived adducts, which should lead to the exclusive formation of bacteriochlorins under thermodynamic conditions.

To rationalise the higher stability of bacteriochlorins with respect to isobacteriochlorins, we analysed their distinct aromatic character. The idealised aromatic pathways of these compounds can be represented as bridged [18]annulene systems, including the macrocyclic 18π-[16]annulene internal cross and the two unsaturated pyrrole systems (Fig. 2). To further validate this scheme, we divided the skeleton of some selected bacteriochlorins (**4**) and isobacteriochlorins (**5** and **5′**) into their corresponding internal cross and the four pyrrolic rings, two of which are saturated.

The aromaticity descriptors evaluated for these compounds were the aromatic ring chemical shieldings (ARCS),[7] the nucleus-independent chemical shieldings (NICS)[8] and the harmonic oscillator model of aromaticity (HOMA)[9] index (see Supplementary data for a detailed description of each method). The ARCS are related to the ring current (I_{ring}) created by cyclic aromatic molecules in the presence of an external magnetic field (B_{ext}). The induced ring-current susceptibility $\delta I_{ring}/\delta B_{ext}$ was estimated by means of the isotropic nuclear magnetic shielding constant σ, calculated at discrete points perpendicular to the molecular plane starting from the geometrical centre of the current loop. We also calculated NICS(0) at the centre of the internal cross and the four pyrrole rings. On the other hand, the HOMA model has been suggested to be the most reliable definition of aromaticity based on the geometric criterion. We calculated the HOMA indexes for the internal cross, and the two unsaturated pyrrolic rings of each evaluated molecule

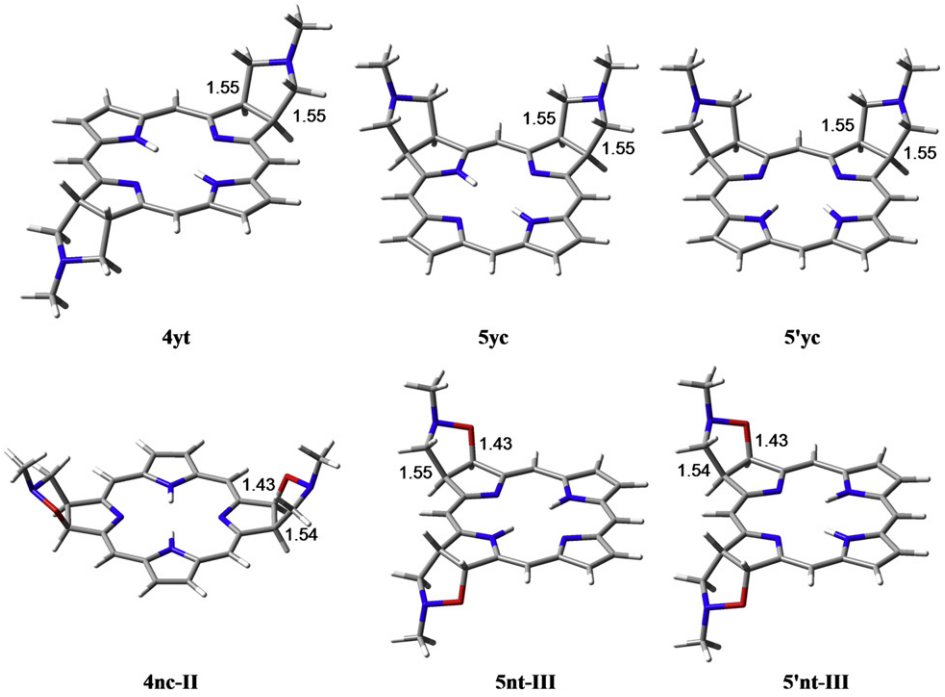

Figure 1. Representative products of the cycloaddition of **2y** with **3y** (up) and of **2n** with **3n** (below), optimised at the B3LYP/6-31G(d) level. Distances are given in angstrom.

(this model is not valid for the non-aromatic pair of β-saturated rings). The results of ARCS, NICS(0) and HOMA calculated for the structures in Figure 1 are gathered in Table 2.

In terms of ARCS, very good agreement was obtained with respect to previously reported values,[6b,7b] the two faces of each planar system being almost identical. As a conclusion, the more stable bacteriochlorins **4** have a more strong aromatic character than isobacteriochlorins **5** and **5′**, as clearly reflected in their higher current susceptibilities and NICS(0) on the centre of the internal cross. These differences follow the same tendency within the geometric HOMA indexes, and this corroborates the direct correspondence between the stability and aromaticity of these compounds. Interestingly, the tautomers of isobacteriochlorins denoted as **5′** appear to be somewhat more aromatic than **5**, exhibiting more important magnetic values, as revealed by higher ARCS and NICS(0) values. This increase in aromaticity counterbalances the higher repulsion between the two neighbouring NH hydrogens, which is referred to be significant.[10] In addition, the pyrrole rings bearing NH groups are clearly more aromatic than the other five-membered rings, and of course much more than the non-aromatic β-saturated ones.

2.2. FMO analysis

The next step in our study was to analyse the frontier molecular orbitals (FMOs) involved in the reactions. It has been reported that, under special conditions, nitrones can participate in inverse electron-demand cycloadditions,[11] but in our particular systems, both reactions with azomethine ylide and *N*-methylnitrone appear to be of normal electron-demand, attending to the relative energy of the FMOs. Remarkably, the LUMO and LUMO+1 of both chlorins, **3y** and **3n**, which differ only in 0.52 and 0.50 eV, respectively, show a reverse preference to receive the electron density of the incoming dipole. Thus, as shown in Figure 3, the LUMO should direct the second cycloaddition to the adjacent pyrrole rings, whereas the LUMO+1 should direct it to the opposite one. Therefore, and following this argument strictly, both approximations should be easily accessible under kinetic conditions and the formation of bacterio- and isobacteriochlorins should be possible with both dipoles.

2.3. Complete reaction pathways calculations

Given that neither thermodynamic nor FMO simple criteria are able to explain the experimental observations, we decided to calculate the whole possible reaction pathways for the two successive 1,3-dipolar cycloadditions of dipoles **2y** and **2n** to porphyrin **1**. A noteworthy good agreement was obtained between the activation parameters reported for several nitrones cycloadditions onto substituted ethylenes[5c] and the values calculated in this work. Thus, $\Delta H^{\ddagger}$ is 16.3 kcal mol^{-1} for the first cycloaddition of nitrone **2n** to porphyrin **1** and ranges between 17.3 and 19.8 kcal mol^{-1} for the successive cycloaddition of **2n** to chlorin **3n**, being the experimental values between 15.7 and 18.3 kcal mol^{-1}. The same accordance was obtained for the calculated values of $\Delta S^{\ddagger}$, which slightly oscillate around -27.8 cal mol^{-1} K^{-1} in all cases (experimental values range between -24.4 and -32.4 cal mol^{-1} K^{-1}). Azomethine ylides are much less stable than nitrones and rarely isolable, so they are typically generated 'in situ' and thus experimental kinetic data for the 1,3-cycloaddition reaction with this substrates are very scarce. On the other hand, these results also agree very well with recent high-level calculations on 1,3-dipolar cycloaddition of nitrones and azomethine ylides to alkenes[12] and hence validate the theoretical method employed in this study. Figure 4 shows the minimum energy paths (MEPs) calculated for these reactions in terms of total free Gibbs (ΔG_{total}) energies (see Section 4.1).

These representations allowed us to establish the exergonic or endergonic character of each process. It must be noted that 1,3-dipolar cycloadditions of azomethine ylide **2y** over porphyrin **1** and its derived chlorin **3y** are clearly irreversible and, consequently, kinetically controlled. On the other hand, cycloadditions of nitrone **2n** over porphyrin **1** and chlorin **3n** are reversible, suggesting that these processes are under thermodynamic control and explaining the poor experimental yields. According to previous observations, the reversibility of the reaction under mild conditions is a common

Table 1
Calculated Gibbs free energies[a] both in the gas phase and in solution, together with the solvation free energies (in kcal mol^{-1}) for the structures described in this work

Structure	ΔG_{gas}[b]	$\Delta\Delta G_{solv}$[c]	ΔG_{total}[d]	$\Delta G^{\ddagger}_{total}$
1	0.0	0.0	0.0	
TS1y	16.5	0.6	17.1	
3y	−36.2	0.4	−35.8	
TS2yc	−17.4	1.3	−16.1	0.5
TS2yt	−17.7	1.3	−16.5	0.2
TS3yc	−17.2	0.6	−16.6	*0.0*
TS3yt	−16.9	0.4	−16.5	0.1
4yc	−69.7	0.9	−68.7	
4yt	−69.9	0.9	−68.9	
5yc	−64.8	0.3	−64.5	
5′yc	−65.1	1.1	−64.0	
5yt	−64.9	0.2	−64.7	
5′yt	−65.3	1.1	−64.2	
TS1n	29.4	1.4	0.0	
3n	−0.2	1.5	30.8	
TS2nc-I	30.4	3.0	1.3	0.1
TS2nc-II	30.3	3.0	33.3	*0.0*
TS2nt-I	30.3	3.0	33.3	*0.0*
TS2nt-II	30.3	3.0	33.3	*0.0*
TS3nc-I	32.9	2.5	33.3	2.1
TS3nc-II	32.5	2.6	35.4	1.9
TS3nc-III	32.9	2.4	35.2	2.0
TS3nt-I	32.7	2.3	35.3	1.8
TS3nt-II	32.7	2.3	35.1	1.7
TS3nt-III	32.8	2.3	35.0	1.9
4nc-I	1.8	3.1	4.8	
4nc-II	1.7	3.1	4.8	
4nt-I	1.6	3.1	4.7	
4nt-II	1.6	3.1	4.6	
5nc-I	7.5	2.7	10.2	
5′nc-I	6.8	3.2	10.0	
5nc-II	7.1	2.7	9.8	
5′nc-II	6.4	3.3	9.7	
5nc-III	7.3	2.5	9.8	
5′nc-III	6.5	3.2	9.7	
5nt-I	7.3	2.5	9.8	
5′nt-I	6.7	2.9	9.6	
5nt-II	7.1	2.4	9.5	
5′nt-II	6.4	3.0	9.4	
5nt-II	7.3	2.3	9.6	
5′nt-III	6.4	3.2	9.6	

[a] Porphyrin and 1,3-dipoles have been arbitrarily chosen as the zero level in the relative energy calculations.
[b] Calculated at the B3LYP/6-31G(d) level.
[c] Calculated at the IEF-PCM/B3LYP/6-31G(d)//B3LYP/6-31G(d) level.
[d] Calculated with Eq. 1 (see Section 4.1).

feature of numerous 1,3-cycloadditions of nitrones with alkenes, whereas pyrrolidines are generally more stable and much less susceptible to undergo 1,3-dipolar cycloreversion to regenerate the azomethine ylides.[5e] This key finding allowed us to locate the source of the experimentally observed difference in site selectivity. Whereas the small energy differences of the TS leading to bacterio- and isobacteriochlorins in the case of the reactions of ylide **2y** (**TS2y** and **TS3y**) are the only responsible of the observed **4y**/**5y** ratio, in the case of the reactions of nitrone **2n**, both the kinetic and the thermodynamic reaction channels lead to the exclusive formation of bacteriochlorins **4n**.

A representative set of TS corresponding to the cycloaddition reactions over chlorins **3y** and **3n** are shown in Figure 5 (all the calculated TSs are available in the Supplementary data). As expected, the two incipient C–C bonds have the same length in **TS2yt**, unlike in the less symmetrical **TS3yc**. On the contrary, the incipient C–C are ca. 0.2 Å longer than incipient C–O bonds in **TS2nc-II** and **TS3nt-III**, due to their distinct electronic nature. As revealed by IRC calculations (see Section 4.1 and Supplementary data) and comparing the structures of these TS with those of the final products (Fig. 1), a high asynchronous character for the nitrone-derived TS is revealed, whereas the synchronicity in **TS2yt** is almost complete. It is worthy to note that some degree of asynchronicity appears on the less symmetrical **TS3yc**, too. As can be seen in these plots, the higher earliness of **TS2yt** and **TS3yc** is revealed by their longer incipient bonds when compared with those of **TS2nc-II** and **TS3nt-III**. According to Hammond's postulate, this earlier character of the ylide-derived TS should be responsible for the low kinetic site selectivity obtained.

The energies of all the calculated structures are gathered in Table 1. As can be seen through these data, calculations show a very poor differentiation between cis and trans approximations (stereoselectivity) in ylide- and nitrone-related cycloadditions, both in the gas phase and in the solution. On the other hand, solvent effects play a key role in the kinetically controlled formation of bacteriochlorins **4y** and isobacteriochlorins **5y** (site selectivity). Consequently, less favourable **TS3yc**,**t** become slightly lower in energy than **TS2yc**,**t** when solvation is taken into account. This situation leads to a global kinetic site selectivity of 39/61 of products **4y** and **5y** (based on the Boltzmann distribution obtained from Gibbs free energies of all TS). This important finding can be correlated with the higher calculated dipole moments in solution of **TS3yc** (μ=7.7 D) and **TS3yt** (μ=7.4 D) when compared with those of **TS2yc** (μ=4.4 D) and **TS2yt** (μ=4.1 D). This results in 'less positive' free solvation energies (including non-electrostatic factors) for the former, that is, to a greater differential stabilisation in solution. However, in the case of the nitrone-derived chlorin **3n**, the differences between the activation barriers leading to bacteriochlorins **4n** and isobacteriochlorins **5n** are greater in the gas phase (around 2 kcal mol^{-1}), and therefore solvent effects have a very small influence on the site selectivity in this case.

2.4. Testing the importance of solvation effects

With the aim of further test the influence of the medium polarity on the dipolar cycloaddition, additional theoretical and experimental explorations of the site selectivity were done. Figure 6 shows the relative activation free Gibbs energies ($\Delta G^{\ddagger}_{total}$) calculated for all **TS2y** and **TS3y** (cis and trans approximations were evaluated separately) as a function of the solvation free energies ($\Delta\Delta G_{solv}$) calculated in several solvents. As can be seen through

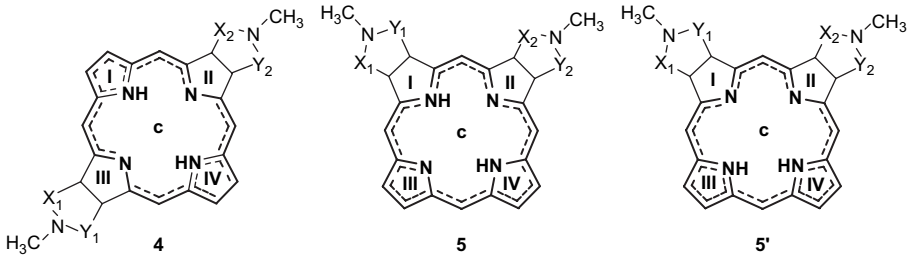

Figure 2. Aromatic pathways for bacterio- and isobacteriochlorins.

Table 2
Induced ring-current susceptibilities (in nAT^{-1}), nuclear-independent chemical shifts (in ppm) and harmonic oscillator model of aromaticity indexes of the representative bacterio- and isobacteriochlorins shown in Figure 1

Structure	$\delta I_{ring}/\delta B_{ext}$[a]	Internal cross (**c**)	NICS(0)[a] [HOMA][b]			
			Ring **I**	Ring **II**	Ring **III**	Ring **IV**
4yt	9.1/9.1	−14.9 [0.942]	−17.1 [0.766]	7.5	7.5	−17.1 [0.766]
5yc	2.9/2.9	−2.7 [0.849]	−0.3	2.1	−6.6 [0.507]	−13.4 [0.843]
5′yc	4.4/4.5	−5.6 [0.919]	3.6	3.6	−13.3 [0.767]	−13.3 [0.767]
4nc-II	9.3/9.3	−15.2 [0.944]	−17.0 [0.759]	7.6	7.6	−17.0 [0.759]
5nt-III	3.1/3.1	−3.2 [0.853]	0.2	2.7	−6.5 [0.503]	−13.7 [0.841]
5′nt-III	4.9/4.9	−6.5 [0.921]	4.2	4.2	−13.7 [0.767]	−13.7 [0.767]

[a] Calculated at the GIAO/HF/6-31+G(d)//B3LYP/6-31G(d) level. The values of $\delta I_{ring}/\delta B_{ext}$ correspond to the top and bottom faces of the planar systems, respectively, as displayed in Figure 1.
[b] Calculated for geometries optimised at the B3LYP/6-31G(d) level.

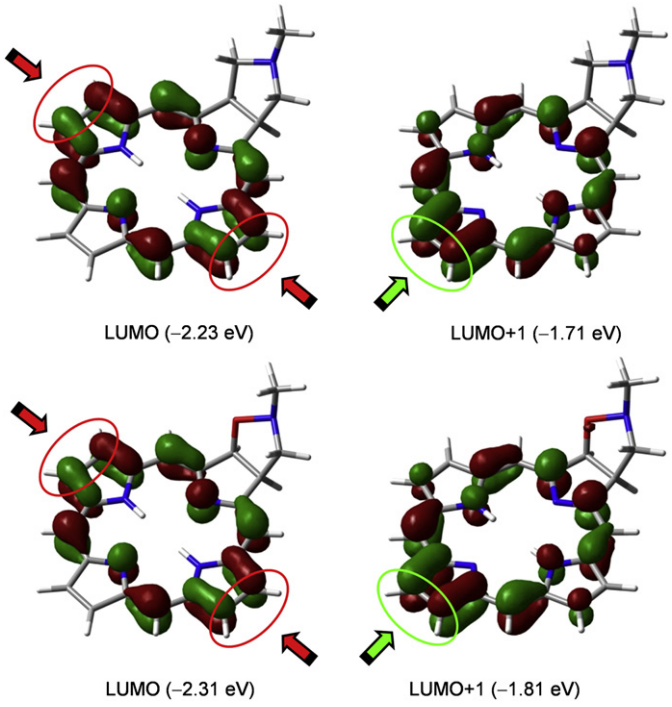

Figure 3. Surface plots of the two first unoccupied molecular orbitals of chlorins **3y** (up) and **3n** (below) calculated at the B3LYP/6-31G(d) level. Coloured arrows indicate the preferred site for the second 1,3-DC reaction.

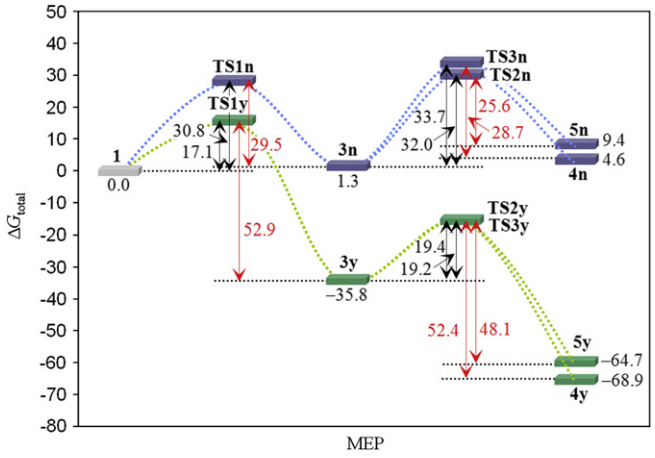

Figure 4. Minimum energy paths in terms of ΔG_{total} (in kcal mol^{-1}) of the successive 1,3-dipolar cycloadditions of **1** with **2y** (green) and **2n** (blue). Reverse activation barriers are displayed in red.

these plots, the use of higher polar solvents results in higher calculated free energies of solvation, which in turn favours the formation of isobacteriochlorins **5y** as major products. These predictions were pleasingly supported by the experimental results. In this sense, the use of DMF, THF and 1,4-dioxane as reaction solvents allowed us to prepare isobacteriochlorins as the exclusive bisadducts, the formation of bacteriochlorins being totally suppressed. The use of 1,2-dichoroethane (1,2-DCE) also led to isobacteriochlorins as the major products, but accompanied with traces of bacteriochlorins. In contrast, the use of toluene led to an equimolecular mixture of bacterio- and isobacteriochlorins.

Despite of the low yields generally obtained in these kinds of reactions, it is worthy to note that the use more polar solvents induces the exclusive formation of isobacteriochlorins whereas the use of less polar solvents gives a mixture of bacterio- and isobacteriochlorins. This fact may help to improve the selective synthesis of either derivative under optimised reaction conditions.

3. Conclusion

A theoretical study has been carried out to explain the different behaviour of azomethine ylide and *N*-methylnitrone in 1,3-dipolar cycloadditions over *meso*-unsubstituted porphyrin. The computational results agree with the experimental observations, that is, the azomethine ylide-derived chlorin **3y** incorporates a second 1,3-dipole mainly to one of the adjacent pyrrole rings, whereas the nitrone-derived chlorin **3n** does it exclusively to the opposite one. This feature is originated by the earlier character of all ylide-related TS with respect to the nitrone-related counterparts, what make the processes in which azomethine ylides are involved to be kinetically controlled. On the contrary, both kinetic and thermodynamic conditions favour the exclusive production of nitrone-derived bacteriochlorins **4n**. Moreover, solvent effects play a key role to favour the formation of the thermodynamically less stable isobacteriochlorins **5y**. In this sense, the simple change of solvent under the same reaction conditions with azomethine ylide, can give rise to a change on the site selectivity going from the exclusive synthesis of isobacteriochlorins to an 1:1 mixture of bacterio- and isobacteriochlorins. This constitutes a new example of the importance of including solvent effects in molecular modelling studies as well as of the synthetic usefulness of the predictions made by the computational mechanistic studies.

4. Experimental section

4.1. Computational details

All calculations were carried out by means of the B3LYP hybrid functional,[13] which has been widely used in theoretical studies of pyrrole macrocycles and porphyrinoid systems with remarkable

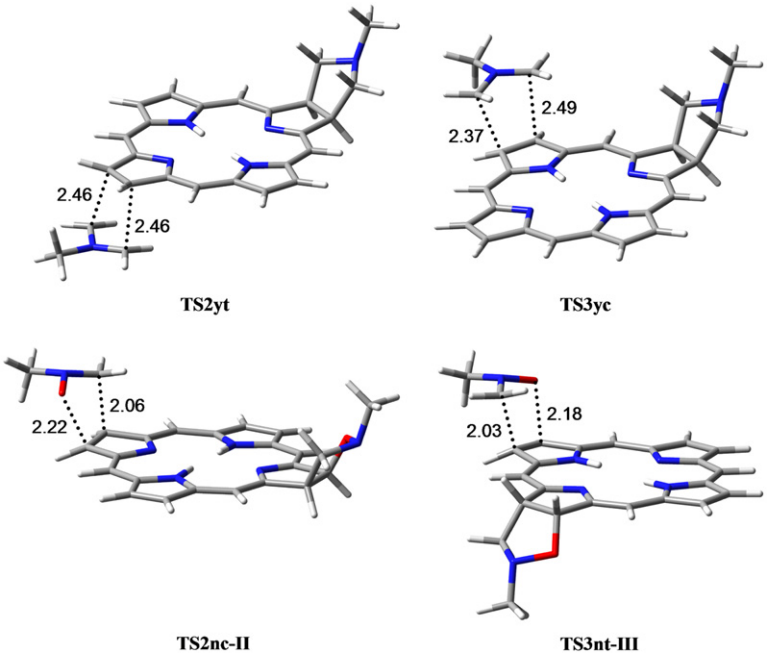

Figure 5. Representative transition structures of the cycloaddition of **2y** with **3y** (up) and of **2n** with **3n** (below), optimised at the B3LYP/6-31G(d) level. Distances of incipient bonds are given in angstrom.

success, both in terms of geometry optimisations and calculation of magnetic properties.[8b,8f,14] Full geometry optimisations and transition structure (TS) searches were carried out in redundant internal coordinates with the 6-31G(d) basis set using the Gaussian 03 package.[15] BSSE corrections have not been considered in this work. Frequency analyses were carried out on the optimised geometries at the same level of theory, and the nature of the stationary points located at the potential energy surface, either minima or transition structures, was determined in each case according to the appropriate number of negative eigenvalues of the Hessian matrix. Scaled frequencies were not considered since significant errors on the calculated thermodynamical properties are not found at this theoretical level.[16] Mass-weighted intrinsic reaction coordinate (IRC) calculations were carried out on structure **TS2nt-II** as an example of reaction path following, by using the Gonzalez and Schlegel scheme.[17] Solvent effects were taken into account throughout the Polarized Continuum Model (IEF-PCM)[18] using UAHF radii, as implemented in Gaussian 03. The internally stored parameters of toluene were used to calculate solvation energies. Only the *exo* approximations in the 1,3-dipolar cycloadditions were fully evaluated because preliminary calculations clearly showed that the *endo* approximations were always much less favourable because of steric repulsions with the porphyrin macrocycle and the bicyclic systems of chlorins.

Zero-point corrected and Gibbs free energies were used for the discussion on the relative stabilities of the considered structures. These energies were obtained by using the following correction formula:

$$\Delta G_{\text{total}} = \Delta E_{\text{elect}} + \Delta G_{\text{temp}} + \Delta\Delta G_{\text{solv}} \quad (1)$$

where ΔE_{elect} is the relative electronic energy calculated at the B3LYP/6-31G(d) level, ΔG_{temp} is the thermal and entropic corrections calculated at 298 K at the B3LYP/6-31G(d) level and $\Delta\Delta G_{\text{solv}}$ is the solvation free energy, calculated at the IEF-PCM/B3LYP/6-31G(d)//B3LYP/6-31G(d) level.

To ensure origin independence in the shielding calculations, the gauge-including-atomic-orbital (GIAO) approach[19] at the HF/6-31+G(d)//B3LYP/6-31G(d) level has been employed to calculate aromaticity magnetic descriptors.

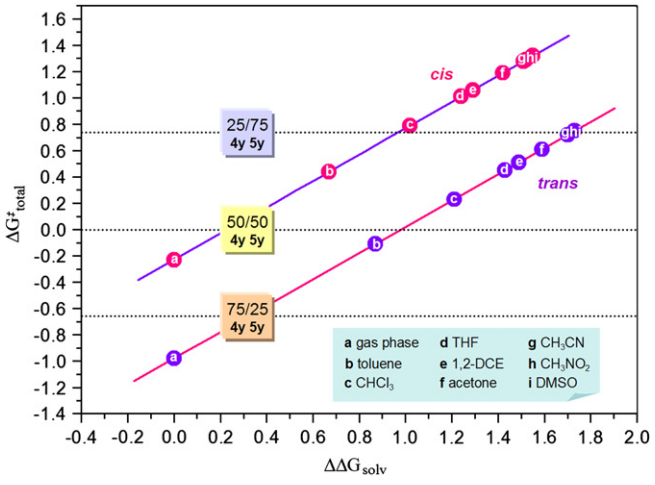

Figure 6. Solvation free energies and activation free Gibbs energies (in kcal mol^{-1}) of **TS2y** and **TS3y**, calculated in several solvents. $\Delta\Delta G_{\text{solv}}$ was calculated at the IEF-PCM/B3LYP/6-31G(d)//B3LYP/6-31G(d) level, and $\Delta G^{\ddagger}_{\text{total}}$ was obtained through Eq. 1 (see Section 4.1). **TS3y** has been arbitrarily chosen as the zero level in the calculation of $\Delta\Delta G_{\text{solv}}$ and $\Delta G^{\ddagger}_{\text{total}}$.

4.2. Reactions with azomethine ylide

A toluene (5 cm^3) solution of *meso*-tetrakis(pentafluorophenyl)porphyrin (22 mg), *N*-methylglycine (4 mg, 2 equiv) and paraformaldehyde (3.4 mg, 5 equiv) was heated at reflux for 5 h under a nitrogen atmosphere. TLC of the reaction mixture showed that about half of the starting porphyrin was converted into two new products. Further portions of *N*-methylglycine (4 mg) and paraformaldehyde (3.4 mg) were then added and the resulting mixture was refluxed for another 5 h. The solvent was evaporated and the corresponding chlorin (14.2 mg, 61%) and one isobacteriochlorin (2.8 mg, 11%) were purified by column chromatography

using a gradient of $CHCl_3$–light petroleum. The influence of the medium polarity was tested by treating the isolated chlorin (21 mg) with *N*-methylglycine (3.8 mg, 2 equiv) and paraformaldehyde (3.2 mg, 5 equiv) in several solvents (DMF, THF, 1,4-dioxane and 1,2-dichloroethane) at 60 °C for 6 h. Conversion (6–16%) and site selectivity data were then measured by ^1H NMR analysis of the reaction mixtures without further purification.

4.3. Reaction with *N*-methylnitrone

meso-Tetrakis(pentafluorophenyl)porphyrin (95 mg), *N*-methylnitrone (4.7 mg, 4 equiv) and toluene (a few drops) were heated under a nitrogen atmosphere in a closed vessel at 60–100 °C for 5 days. After cooling to rt, the resulting residue was purified by flash chromatography using a mixture of cyclohexane/dichloromethane (2:3) as eluent to obtain the corresponding chlorin (60 mg, 72%). The fraction of the bacteriochlorins (10 mg, 16%) was further purified by preparative TLC using toluene/ethyl acetate (99:1) as eluent. As in the reactions with azomethine ylide, no secondary reactions were observed, and therefore only the unreacted starting material and the corresponding bacterio- and isobacteriochlorins were detected.

Acknowledgements

This work was supported by the Ministerio de Ciencia y Tecnología (projects CTQ2005-08016 and Consolider Ingenio 2010 CSD2006-00), the University of Aveiro, the Fundação para a Ciência e a Tecnologia (grant SFRH/BPD/8374/2002 of A.M.G.S.) and FEDER for funding the Organic Chemistry Research Unit. Authors gratefully thank Prof. J. Elguero for his valuable comments and CESGA for computer support.

Supplementary data

Hard data on Cartesian coordinates, electronic energies, as well as entropies, enthalpies, Gibbs free energies and lowest frequencies of all structures considered are available free of charge as Supplementary data in the online version of the paper. Supplementary data associated with this article can be found in the online version, at doi:10.1016/j.tet.2008.06.018.

References and notes

1. (a) Bonnett, R. *Chemical Aspects of Photodynamic Therapy*; Gordon and Breach Science: Australia, 2000; p 177; (b) Pandey, R. K.; Zheng, G. Porphyrins as Photosensitizers in Photodynamic Therapy. In *The Porphyrin Handbook*; Kadish, K. M., Smith, K. M., Guilard, R., Eds.; Academic: San Diego, 2000; Vol. 6, Chapter 43; (c) *Photodynamic Tumour Therapy – 2nd and 3rd Generation Photosensitizers*; Moser, J. G., Ed.; Harwood Academic: Amsterdam, 1998; (d) Bonnett, R. *Chem. Soc. Rev.* **1995**, *24*, 19–33; (e) Sternberg, E. D.; Dolphin, D.; Brückner, C. *Tetrahedron* **1998**, *54*, 4151–4202.
2. (a) Silva, A. M. G.; Tomé, A. C.; Neves, M. G. P. M. S.; Silva, A. M. S.; Cavaleiro, J. A. S. *Chem. Commun.* **1999**, 1767–1768; (b) Silva, A. M. G.; Tomé, A. C.; Neves, M. G. P. M. S.; Silva, A. M. S.; Cavaleiro, J. A. S. *J. Org. Chem.* **2005**, *70*, 2306–2314; (c) Silva, A. M. G.; Tomé, A. C.; Neves, M. G. P. M. S.; Cavaleiro, J. A. S.; Perrone, D.; Dondoni, A. *Synlett* **2005**, 857–859.
3. (a) Tomé, A. C.; Lacerda, P. S. S.; Silva, A. M. G.; Neves, M. G. P. M. S.; Cavaleiro, J. A. S. *J. Porphyrins Phthalocyanines* **2000**, *4*, 532–537; (b) Silva, A. M. G.; Tomé, A. C.; Neves, M. G. P. M. S.; Silva, A. M. S.; Cavaleiro, J. A. S.; Perrone, D.; Dondoni, A. *Tetrahedron Lett.* **2002**, *43*, 603–605.
4. Some examples: (a) Desjardins, A.; Flemming, J.; Sternberg, E. D.; Dolphin, D. *Chem. Commun.* **2002**, 2622–2623; (b) Flemming, J.; Dolphin, D. *Tetrahedron Lett.* **2002**, *43*, 7281–7283; (c) DiNello, R. K.; Dolphin, D. *J. Org. Chem.* **1980**, *45*, 5196–5204; (d) Morgan, A. R.; Pangka, V. S.; Dolphin, D. *J. Chem. Soc., Chem. Commun.* **1984**, 1047–1048; (e) Pangka, V. S.; Morgan, A. R.; Dolphin, D. *J. Org. Chem.* **1986**, *51*, 1094–1100; (f) Yong-Hin, P.; Wijesekera, T. P.; Dolphin, D. *Tetrahedron Lett.* **1989**, *30*, 6135–6138; (g) Morgan, A. R.; Kohli, D. H. *Tetrahedron Lett.* **1995**, *36*, 7603–7606; (h) Faustino, M. A. F.; Neves, M. G. P. M. S.; Vicente, M. G. H.; Silva, A. M. S.; Cavaleiro, J. A. S. *Tetrahedron Lett.* **1996**, *37*, 3569–3570; (i) Callot, H. J.; Johnson, A. W.; Sweeney, A. *J. Chem. Soc., Perkin Trans. 1* **1973**, 1424–1427; (j) Cavaleiro, J. A. S.; Jackson, A. H.; Neves, M. G. P. M. S.; Rao, K. R. N. *J. Chem. Soc., Chem. Commun.* **1985**, 776–777; (k) Yong-Hin, P.; Wijesekera, T. P.; Dolphin, D. *Tetrahedron Lett.* **1991**, *32*, 2875–2878; (l) Pandey, R. K.; Shiau, F.-Y.; Ramachandran, K.; Dougherty, T. J.; Smith, K. M. *J. Chem. Soc., Perkin Trans. 1* **1992**, 1377–1385; (m) Maeda, C.; Yamaguchi, S.; Ikeda, C.; Shinokubo, H.; Osuka, A. *Org. Lett.* **2008**, *10*, 549–552; (n) Tanaka, T.; Nakamura, Y.; Osuka, A. *Chem.—Eur. J.* **2008**, *14*, 204–211; (o) Tanaka, T.; Nakamura, Y.; Aratani, N.; Osuka, A. *Tetrahedron Lett.* **2008**, *49*, 3308–3311.
5. Recent reviews and books: (a) Pandey, G.; Banerjee, P.; Gadre, S. R. *Chem. Rev.* **2006**, *106*, 4484–4517; (b) Rück-Braun, K.; Freysoldt, T. H. E.; Wierschem, F. *Chem. Soc. Rev.* **2005**, *34*, 507–516; (c) Tufariello, J. J. *1,3-Dipolar Cycloaddition Chemistry*; Padwa, A., Ed.; Wiley: New York, NY, 1984; Vol. 2; (d) Lown, J. W. *1,3-Dipolar Cycloaddition Chemistry*; Padwa, A., Ed.; Wiley: New York, NY, 1984; Vol. 1; (e) Bianchi, G.; Gandolfi, R. *1,3-Dipolar Cycloaddition Chemistry*; Padwa, A., Ed.; Wiley: New York, NY, 1984; Vol. 2; (f) Torssell, K. B. G. *Nitrile Oxides, Nitrones and Nitronates in Organic Synthesis*; VCH: New York, NY, 1988.
6. (a) Ghosh, A.; Lü, T. X.; Almlöf, J. *J. Phys. Chem.* **1995**, *99*, 1073–1075; (b) Reimers, J. R.; Lü, T. X.; Crossley, M. J.; Hush, N. S. *J. Am. Chem. Soc.* **1995**, *117*, 2855–2861; (c) Boronat, M.; Ortí, E.; Viruela, P. M.; Tomás, F. *J. Mol. Struct. (Theochem)* **1997**, *390*, 149–156; (d) Ghosh, A. *Acc. Chem. Res.* **1998**, *31*, 189–198 and references cited therein.
7. (a) Jusélius, J.; Sundholm, D. *Phys. Chem. Chem. Phys.* **1999**, *1*, 3429–3435; (b) Jusélius, J.; Sundholm, D. *Phys. Chem. Chem. Phys.* **2000**, *1*, 2145–2151; (c) Jusélius, J.; Sundholm, D. *J. Org. Chem.* **2000**, *65*, 5233–5237.
8. (a) Schleyer, P. V. R.; Maerker, C.; Dransfield, A.; Jiao, H.; Van Eikema Hommes, N. J. R. *J. Am. Chem. Soc.* **1996**, *118*, 6317–6318; (b) Cyránski, M. K.; Krygowski, T. M.; Wisiorowski, M.; Van Eikema Hommes, N. J. R.; Schleyer, P. V. R. *Angew. Chem., Int. Ed.* **1998**, *37*, 177–180; (c) Schleyer, P. V. R.; Monohar, M.; Wang, Z.; Kiran, B.; Jiao, H.; Puchta, R.; van Eikema Hommes, N. J. R. *Org. Lett.* **2001**, *3*, 2465–2468; (d) Corminboeuf, C.; Heine, T.; Seifert, G.; Schleyer, P. V. R.; Weber, J. *Phys. Chem. Chem. Phys.* **2004**, *6*, 273–276; (e) Krygowski, T. M.; Ejsmont, K.; Stepien, B. T.; Cyránski, M. K.; Poater, J.; Solà, M. *J. Org. Chem.* **2004**, *69*, 6634–6640; (f) Furuta, H.; Maeda, H.; Osuka, A. *J. Org. Chem.* **2001**, *66*, 8563–8572.
9. (a) Krygowski, T. M. *J. Chem. Inf. Comput. Sci.* **1993**, *33*, 70–78; (b) Krygowski, T. M.; Cyránski, M. K. *Tetrahedron* **1996**, *52*, 1713–1722; (c) Krygowski, T. M.; Cyránski, M. K. *Tetrahedron* **1996**, *52*, 10255–10264.
10. Schlabach, M.; Scherer, G.; Limbach, H.-H. *J. Am. Chem. Soc.* **1991**, *113*, 3550–3558.
11. Shindo, M.; Itoh, K.; Tsuchiya, C.; Shishido, K. *Org. Lett.* **2002**, *4*, 3119–3121 and references cited therein.
12. Ess, D. H.; Houk, K. N. *J. Phys. Chem. A* **2005**, *109*, 9542–9553.
13. (a) Lee, C.; Yang, W.; Parr, R. *Phys. Rev. B* **1988**, *37*, 785–789; (b) Becke, A. D. *J. Chem. Phys.* **1993**, *98*, 5648–5652.
14. (a) Islyaikin, M. K.; Ferro, V. R.; García de la Vega, J. M. *J. Chem. Soc., Perkin Trans. 2* **2002**, 2104–2109; (b) Ferro, V. R.; García de la Vega, J. M.; González-Jonte, R. H.; Poveda, L. A. *J. Mol. Struct. (Theochem)* **2001**, *537*, 223–224; (c) Ferro, V. R.; Claessens, G. G.; González-Jonte, R. H.; García de la Vega, J. M. *Int. J. Quantum Chem.* **2003**, *91*, 369–375; (d) Kobayashi, N.; Ishizaki, T.; Ishii, K.; Konami, H. *J. Am. Chem. Soc.* **1999**, *121*, 9096–9110; (e) Ghosh, A. *J. Porphyrins Phthalocyanines* **2000**, *4*, 380–381 and references cited therein; (f) Parusel, A. B. J.; Wondimagegn, T.; Ghosh, A. *J. Am. Chem. Soc.* **2000**, *122*, 6371–6374.
15. Frisch, M. J.; Trucks, G. W.; Schlegel, H. B.; Scuseria, G. E.; Robb, M. A.; Cheeseman, J. R.; Montgomery, J. A., Jr.; Vreven, T.; Kudin, K. N.; Burant, J. C.; Millam, J. M.; Iyengar, S. S.; Tomasi, J.; Barone, V.; Mennucci, B.; Cossi, M.; Scalmani, G.; Rega, N.; Petersson, G. A.; Nakatsuji, H.; Hada, M.; Ehara, M.; Toyota, K.; Fukuda, R.; Hasegawa, J.; Ishida, M.; Nakajima, T.; Honda, Y.; Kitao, O.; Nakai, H.; Klene, M.; Li, X.; Knox, J. E.; Hratchian, H. P.; Cross, J. B.; Bakken, V.; Adamo, C.; Jaramillo, J.; Gomperts, R.; Stratmann, R. E.; Yazyev, O.; Austin, A. J.; Cammi, R.; Pomelli, C.; Ochterski, J. W.; Ayala, P. Y.; Morokuma, K.; Voth, G. A.; Salvador, P.; Dannenberg, J. J.; Zakrzewski, V. G.; Dapprich, S.; Daniels, A. D.; Strain, M. C.; Farkas, O.; Malick, D. K.; Rabuck, A. D.; Raghavachari, K.; Foresman, J. B.; Ortiz, J. V.; Cui, Q.; Baboul, A. G.; Clifford, S.; Cioslowski, J.; Stefanov, B. B.; Liu, G.; Liashenko, A.; Piskorz, P.; Komaromi, I.; Martin, R. L.; Fox, D. J.; Keith, T.; Al-Laham, M. A.; Peng, C. Y.; Nanayakkara, A.; Challacombe, M.; Gill, P. M. W.; Johnson, B.; Chen, W.; Wong, M. W.; Gonzalez, C.; Pople, J. A. *Gaussian 03, Revision C.02*; Gaussian: Wallingford, CT, 2004.
16. (a) Bauschlicher, C. W., Jr. *Chem. Phys. Lett.* **1995**, *246*, 40–44; (b) Scott, A. P.; Radom, L. *J. Phys. Chem.* **1996**, *100*, 16502–16513.
17. (a) Gonzalez, C.; Schlegel, H. B. *J. Chem. Phys.* **1989**, *90*, 2154–2161; (b) Gonzalez, C.; Schlegel, H. B. *J. Chem. Phys.* **1990**, *94*, 5523–5527.
18. (a) Cossi, M.; Barone, V.; Mennucci, B.; Tomasi. *J. Chem. Phys. Lett.* **1998**, *286*, 253–260; (b) Tomasi, J.; Mennucci, B.; Cancès, E. *J. Mol. Struct. (Theochem)* **1999**, *464*, 211–226; (c) Cossi, M.; Scalmani, G.; Rega, N.; Barone, V. *J. Chem. Phys.* **2002**, *117*, 43–54 and references cited therein.
19. (a) London, F. *J. Phys. Radium* **1937**, *8*, 397–409; (b) Hameka, H. *Mol. Phys.* **1958**, *1*, 203–215; (c) Ditchfield, R. *Mol. Phys.* **1974**, *27*, 789–807; (d) Wolinski, K.; Hinton, J. F.; Pulay, P. *J. Am. Chem. Soc.* **1990**, *112*, 8251–8260.